DRFC/CAD EUR-CEA-FC 1570

Ordinary mode reflectometry: Modification of the scattering and cut-off responses due to the shape of localized density fluctuations

C. Fanack, I. Boucher, F. Clairet*,
S. Heuraux, G. Leclert and X.L. Zou*

Janvier 1996

CEA EURATOM

ASSOCIATION EURATOM-CEA
DEPARTEMENT DE RECHERCHES
SUR LA FUSION CONTROLEE
CEN/CADARACHE
F-13108 SAINT PAUL LEZ DURANCE CEDEX

Ordinary mode reflectometry: Modification of the scattering and cut-off responses due to the shape of localized density fluctuations

C. Fanack, I. Boucher, F. Clairet*, S. Heuraux, G. Leclert and X.L. Zou*
Laboratoire de Physique des Milieux Ionisés, URA CNRS 835,
Université Henri Poincaré, Nancy I, BP 239, 54506 Vandœuvre Cedex, France
*DRFC, CEA Cadarache, 13108 St Paul-lez-Durance Cedex, France

Abstract

Ordinary wave reflectometry in a plasma containing a localized density perturbation is studied with a 1-D model. The phase response is studied as a function of the wavenumber and position of the perturbation. It is shown that it strongly depends upon the perturbation shape and size. For a small perturbation wavenumber, the response is due to the oscillation of the cut-off layer. For larger wavenumbers, two regimes are found : for a broad perturbation, the phase response is an image of the perturbation itself; for a narrow perturbation, it is rather an image of the Fourier transform. These features are enhanced for a broadband perturbation (modulated square wave) and scattering can occur over the whole region up to the cut-off. The phase response obtained for a damped square perturbation is in excellent agreement with the results of an earlier experiment (Rhodes et al, Phys. Fluids 1992) whereas the Gaussian pulse cannot reproduce them. For tokamak plasmas it turns out that, for the fluctuation spectra usually observed, the phase response comes primarily from those fluctuations that are localized at the cut-off. Finally, the results of a 2-D numerical model show that geometry effects are negligible for the scattering by radial fluctuations.

PACS numbers: 52.40.Db, 52.70.Gw, 07.60.Hv

I. Introduction

The ordinary mode reflectometry is a diagnostic method widely used to measure density profiles in tokamaks (Manso 1993). The local density at the cut-off layer can, in principle, be deduced from the phase of the reflected signal. The density profile is then reconstructed by sweeping the incident frequency (Simonet 1985). In many cases, due to the existence of density fluctuations along the whole beam path between the plasma boundary and the cut-off layer, large errors may occur in the reconstructed profile. Besides, reflectometry is also used for the study of the density fluctuations themselves. Specific experiments in tokamaks have been set up to characterize these fluctuations (Hanson *et al* 1992, Kramer *et al* 1993). The localization of the phase response due to fluctuations, however, is still an open question. Early results are based on the hypothesis that the signal comes primarily from the cut-off layer. In the scattering model introduced more recently, the phase variation arises essentially from the backscattering of the incident wave (whose local wavenumber is $k(x)$) by density fluctuations with a wavenumber k_f at that particular location where the Bragg resonant rule $k_f = 2k(x)$ is satisfied. This has been shown in the one-dimensional case either analytically (Zou *et al* 1991, Bretz 1992) or numerically (Hutchinson 1992). For a perturbation moving down the density gradient from behind the cut-off, and a fixed frequency reflectometer, the Bragg rule predicts that the phase response occurs with a delay depending upon the fluctuation wavenumber : the higher the wavenumber, the larger the delay. In an experiment (Rhodes *et al* 1992) designed to decide between these two possibilities, it was found that the phase response was localized at the cut-off for any value of the fluctuating wavenumber. It was suggested that this localization, in disagreement with the scattering model could result from multidimensional effects, and 2D codes (Irby *et al* 1993) have been developed. However, the 2D numerical results corroborate the scattering model and do not reproduce the experimental results.

The aim of the present work is to analyze the role of the various physical processes involved in the interaction of the incident wave with the density fluctuations. One can then understand the evolution of the phase response as the perturbation moves through the plasma. Basically, there are two distinct processes. First, when the perturbation is close to the cut--off layer, it produces an oscillation of its position; this is the dominant effect for small values of k_f. Second, if the Bragg selection rule is satisfied at a given point, resonant backscattering occurs. For a localized perturbation, which has a finite spectral width, the shape and size of the perturbation play an essential role in the phase response.

The outline of the paper is the following. In section 2, we briefly recall the basic equations of O-mode reflectometry and the characteristics of the 1-D code used to solve them. Localized perturbations with different shapes and sizes are introduced in Section 3 to demonstrate the relative importance of the above mentioned processes. Section 4 shows how the damping modifies the phase response. The results of the experiment of Rhodes *et al* (1992) are then shown to agree with the predictions of the model when these shape and damping effects are properly included. In Section 5, the case of tokamak

plasmas is shortly discussed. Finally, two-dimensional effects are investigated in Section 6. It is found that there is very little difference between the 1-D and 2-D results for radial fluctuations.

2. O-mode reflectometry : basic equations and numerical model.

An incident wave with frequency ω and an ordinary polarization (electric field parallel to the external magnetic field) which propagates into an inhomogeneous plasma satisfies the Helmholtz equation

$$\left[\frac{d^2}{dx^2} + k_0^2\, N_O^2(x)\right] E(x) = 0 \qquad (1)$$

$k_0 = \omega/c$ is the vacuum wavenumber and $N_O(x)$ the refractive index of the ordinary wave

$$N_O^2(x) = 1 - \frac{\omega_{pe}^2(x)}{\omega^2} \qquad (2)$$

$\omega_{pe}(x) = [e^2 n_e(x)/(\varepsilon_o m_e)]^{1/2}$ is the unperturbed plasma frequency and $n_e(x)$ the unperturbed electron density. The incident wave propagates through the plasma up to the cut-off layer where it is reflected. Let $n_{cr} = \varepsilon_o m_e \omega^2/e^2$ the value of the density at the cut-off. In the presence of a density perturbation $\delta n(x)$, Eq. (2) becomes

$$N_O^2(x) = 1 - \frac{n_e(x) + \delta n(x)}{n_{cr}} \qquad (3)$$

For the sake of simplicity, we assume that the unperturbed density has a linear profile

$$\frac{n_e(x)}{n_{cr}} = 1 - \frac{x}{L} \qquad (4)$$

where L is the density gradient length. The cut-off is at $x = 0$ and the propagating side of the plasma corresponds to $x > 0$. When there are no fluctuations, the solution of Eq. (1) is the Airy fonction. In the framework of the Born approximation, it is then possible to express the scattered field and the phase response in terms of Airy fonctions (Zou *et al.* 1991, Afeyan *et al.* 1995).

According to the short discussion of the introduction, two types of localized perturbations will be studied, namely, a Sine wave with either a Gaussian shape (see Fig. 1a) or a square shape (a wavetrain, see Fig. 1b)

$$\delta n(x) = \delta n_0 \exp[-(x - x_f)^2/w_f^2] \cos[k_f(x - x_f)], \qquad (5a)$$

$$\delta n(x) = \begin{cases} \delta n_0 \sin[k_f(x - x_f)] & |x - x_f| \le w_f \\ 0 & |x - x_f| > w_f \end{cases} \qquad (5b)$$

Here w_f is the half-width of the perturbation centered around x_f and k_f is the fluctuating wavenumber. δn_0 is the perturbation amplitude. The essential difference between the two signals lies in the very different behaviour of their spectra. The spectrum of the Gaussian is a Gaussian (Fig. 1c), whereas the spectrum of the wavetrain (Fig.1d) is a cardinal function $\sin(k)/k$, which has significant secondary peaks. It will be seen later that these peaks modify the phase response due to the scattering process.

Equation (1) with both types of perturbed density has been solved numerically. The numerical procedure uses a finite difference scheme based on a fourth order Numerov method. The resulting linear system has been solved by two different methods (Carnahan *et al* 1969), either a Runge-Kutta or a tridiagonal algorithm, with no significant difference. The numerical grid has a length of a few hundreds up to a thousand wavelengths, and a resolution of several hundreds points per wavelength. The phase of the total signal at a given location outside the plasma is computed as a function of the position x_f of the perturbation center. This representation can also be understood as the time evolution of the phase for perturbations moving at a constant speed v, since $x_f = vt$. The time origin corresponds to the perturbation centered at the cut-off.

3. Physical processes: cut-off oscillation, scattering with envelope effects.

The study is restricted in this work to small amplitude perturbations, $\delta n_0/n_{cr} = 0.001$. The effect of large amplitude perturbations is defered to another paper. In order to clearly separate the different physical processes, various values of the parameters (density gradient length, width and wavenumber of the perturbation) will be chosen.

3.1. Small wavenumbers, $k_f \ll k_0$: cut-off oscillation.

Let us consider first the case of fluctuations with small wavenumber relative to k_0, $k_f = 0.04k_0$. We choose a large density gradient length, $L = 1000\lambda_0$ ($\lambda_0 = 2\pi/k_0$ is the vacuum wavelength). The perturbation half-width w_f is $50\lambda_0$.

Figures 2 and 3 give the phase response for the Gaussian and square respectively. The dominant effect is the cut-off oscillation when the perturbation crosses the cut-off layer. In other words, the phase response is localized at the cut-off. This localization of the effect of long wavelength perturbations has been mentioned by Mazzucato *et al.* (1991). The main features of the phase variation have been already reported by Bretz (1992). There is no Bragg scattering in this case. Indeed, by continuity with the WKB region, it is possible to define a local incident wavenumber even near the cut-off

$$k_i(\xi) = \frac{1}{\pi} \left(k_0^{2/3} L^{-1/3}\right) \left(\mathrm{Ai}^2(\xi) + \mathrm{Bi}^2(\xi)\right)^{-1} \qquad (6)$$

where Ai, Bi are the Airy functions and ξ the normalized abscissa, $\xi = xk_0^{2/3}L^{-1/3}$. In contradistinction with the WKB approximation where the wavenumber vanishes at the cut-off ($\xi = 0$), Eq. (6) leads to a finite value called the Airy wavenumber

$$k_A = 0.63\ k_0^{2/3} L^{-1/3} \qquad (7)$$

The present case implies $k_f < 2\ k_A = 0.068\ k_0$, which can be viewed as the minimum value for the fluctuation wavenumber selected by the Bragg resonant rule in the plasma. Therefore the Bragg condition can never be satisfied in the whole propagation region for this k_f. In this case the only physical effect that occurs is phase modulation due to the oscillation of the cut-off layer. The modulation wavelength of the phase response corresponds to the perturbation wavelength. An approximate expression of the phase shift can be derived from the perturbation of the refractive index under the WKB assumption

$$\Delta\Phi_{max} \approx F\ 2\pi \frac{\delta n_0}{n_{cr}} \left(\frac{L/\lambda_0}{k_f/k_0}\right)^{1/2} \qquad (8)$$

where F is a numerical factor of the order of 1 ($F = 0.91$ for a wavetrain). An expression closely related to Eq. (8) is found in Bretz *et al.* (1992). The scaling of the phase with the gradient length L and the wavenumber k_f is well reproduced by numerical computations.

3.2. Large wavenumbers, $2k_A < k_f < 2k_0$: "spectral" and "spatial" regimes of Bragg scattering.

We now consider a gradient length $L = 1000\lambda_0$ and a Gaussian perturbation with a larger wavenumber, $k_f = 0.4k_0 \gg 2k_A$, so we expect that Bragg scattering is the dominant process. As discussed below and shown in details in Appendix A, there are in fact two very distinct behaviours, depending on whether the half-width of the perturbation is larger or smaller than a critical length

$$w_c^2 = \frac{Lk_f}{k_0^2} \qquad (9)$$

For the present set of parameters, $w_c \approx 4\lambda_0$.

3.2.a Gaussian perturbation: spatial case, $w_f > w_c$

- Let us choose a perturbation with a large half-width, namely $w_f = 15\lambda_0$. Figure 4a shows the phase response as a function of x_f. It is clear that the phase response has the same width ($30\lambda_0$) as the perturbation itself. Furthermore, its maximum is at the Bragg position x_B such that $(x_B/L) = k_f^2/(4k_0^2)$ and the modulation length is constant and equal to $2\pi/k_f$. Asymptotic methods can give an approximate analytical expression of the phase response (see Appendix A)

$$\Delta\phi \approx -\pi^{1/2} \frac{k_0 L^{1/2}}{k_f^{1/2}} \frac{\delta n_0}{n_{cr}} \exp\left[-\frac{(x_f - x_B)^2}{w_f^2}\right] \sin(k_f x_f + \psi_0) \qquad (10)$$

$$\psi_0 = \frac{4}{3} k_0 L^{-1/2} x_B^{3/2} - k_f x_B + \pi/4$$

Eq. (10) reproduces qualitatively and quantatively the features of the phase response. This can be easily understood in terms of resonant scattering. A wide perturbation has a narrow wavenumber

spectrum $S(\chi)$ centered around k_f, hence the scattering can only occur for $\chi \approx k_f$, that is at a single point $x = x_B$ in the plasma. The phase response thus oscillates with the constant wavelength $2\pi/k_f$. Its amplitude is maximum when $x_f = x_B$ and decreases like the perturbation amplitude itself. The phase response reproduces the *spatial* features of the perturbation. This case corresponds to the situation studied by Afeyan *et al* (1995) in normalized coordinates. The maximum phase shift is

$$\Delta\phi_{max} \approx \pi\sqrt{2}\left(\frac{L/\lambda_0}{k_f/k_0}\right)^{1/2}\frac{\delta n_0}{n_{cr}} \tag{11}$$

Since k_f/k_0 cannot vary much ($2k_A < k_f < 2k_0$), the important parameter is thus the gradient length.

3.2.b Gaussian perturbation: spectral case, $w_f \ll w_c$

- Let us now consider the opposite case, say $w_f = 2.5\lambda_0$. The results are reported on Fig. 4b. The width is now much larger than the width of the perturbation. The modulation length depends on the position x_f of the perturbation. These results are well reproduced by the appropriate asymptotic evaluation of the phase shift (see Appendix A)

$$\Delta\phi = -\frac{\pi^{1/2}}{2}k_0 w_f\frac{\delta n_0}{n_{cr}}\left(\frac{L}{x_f}\right)^{1/2}\exp\left[-\frac{k_0^2 w_f^2}{L}\left(x_f^{1/2}-x_B^{1/2}\right)^2\right]\sin\left(\frac{4}{3}\frac{k_0}{L^{1/2}}x_f^{3/2}\right) \tag{12}$$

Again, the phase response can be understood in terms of Bragg scattering. As the wavenumber spectrum of the perturbation is large, any component χ of the spectrum can resonantly scatter the incident wave at a position x, possibly far from the Bragg position x_B such that

$$\chi = 2k_0 N_0(x) = 2k_0\sqrt{x/L} \tag{13}$$

The importance of this scattering depends upon the amplitude of the χ-component of the Fourier spectrum of the perturbation. Hence, the phase response is an image of this Fourier spectrum, a Gaussian of half-width $2/w_f$ (in the χ-space) which is distorted in the real space by the nonlinear mapping $\chi \rightarrow x$ set by Eq. (13). The phase response reproduces the *spectral* features of the perturbation. Furthermore, Eq.(13) gives the local modulation length of the phase response. Due to the swelling effect of the incident field expressed by the function $(L/x_f)^{1/2}$, the maximum response is no longer at x_B, but at a slightly lower value. The maximum phase shift can still be estimated with $x_f \approx x_B$

$$\Delta\phi_{max} \approx 2\pi^{3/2}\frac{k_0}{k_f}\frac{w_f}{\lambda_0}\frac{\delta n_0}{n_{cr}} \tag{14}$$

Hence, it is proportional to the perturbation width and does not depend on the gradient length.

The limit between the two regimes, as given by $w_f = w_c$ (see Eq. (9)) corresponds in fact to a perturbation having a width equal to the width [in the x-space, as defined by Eq. (13)] of its spectrum. The results shown on Fig. 4 show that the asymptotic expressions are valid even for w_f not very different from w_c (i.e. 15 and 2.5 compared to 4).

3.2.c. Case of the square perturbation

From the above discussion, one can expect that the pecularities of the spectral case are strongly enhanced for the case of a modulated square. In order to distinguish phenomena near the cut-off and near the usual Bragg position x_B, we choose $L = 1000\lambda_0$ and $k_f = 0.6k_0$. The case of a wide pulse, $w_f = 30\lambda_0$ is shown on Figure 5a. The phase response reproduces the spatial shape of the perturbation, that is, the amplitude stays roughly constant as long as the Bragg position x_B is in the pulse. However, in contradistinction with the Gaussian case, spectral effects occur at the edges, due to the sharp boundaries. For narrow pulses, $w_f = 5\lambda_0$, $k_f = 0.6k_0$, the spectrum shape $\sin(\chi - k_f)/(\chi - k_f)$ is clearly reproduced on Figure 5b. The spectral decay much slower than for the Gaussian case produces significant scattering far from x_B.

In both cases, the existence of sharp boundaries causes the occurence of a significant response near the cut-off. Indeed, whatever the perturbation width is, these sharp edges always give a spectral contribution. A detailed study for this case ($x_f \approx x_c$) shows (Appendix B) that the phase response is

$$\Delta\Phi \approx (4\pi^2)^{2/3} \frac{\delta n_0}{n_{cr}} \frac{k_0}{k_f} \left(\frac{L}{\lambda_0}\right)^{1/3} \mathrm{Ai}^2\left(\frac{x_f k_0^{2/3}}{L^{1/3}}\right) \qquad (15)$$

This Ai^2-like variation is well reproduced on Figure 5a.

In conclusion, we emphasize that, for narrow signals whose spectrum is decaying slowly, a significant part of the energy can be scattered far from the Bragg theoretical position x_B, there is no longer localization of the scattering process. On the other hand, for truely localized signals (which are switched on at a given time) a significant response occurs at the cut-off. When this response is dominant, the scattering process becomes localized, not at the Bragg position but at the cut-off. The maximum phase shift for various regimes can be summarized in Table 1.

Phase Modulation $k_f < 2k_A$	Bragg (WKB region) $2k_A < k_f < 2k_0$ (Gaussian)		Bragg (cut-off) $2k_A < k_f$ (Square)
	Spatial regime	Spectral regime	Sharp edge effects
	$w_f^2 > \frac{Lk_f}{k_0^2}$	$w_f^2 < \frac{Lk_f}{k_0^2}$	
$F2\pi \left(\frac{L/\lambda_0}{k_f/k_0}\right)^{1/2} \times \frac{\delta n_0}{n_{cr}}$	$\sqrt{2}\pi \left(\frac{L/\lambda_0}{k_f/k_0}\right)^{1/2} \times \frac{\delta n_0}{n_{cr}}$	$2\pi^{3/2} \frac{k_0}{k_f} \frac{w_f}{\lambda_0} \times \frac{\delta n_0}{n_{cr}}$	$0.29(4\pi^2)^{2/3} \frac{k_0}{k_f} \left(\frac{L}{\lambda_0}\right)^{1/3} \times \frac{\delta n_0}{n_{cr}}$

Table 1. Maximum phase shift $\Delta\phi_{max}$ for various cases of Section 3 (Eqs. (8), (11), (14) & (15))

4. Damping effect. Comparison with the experimental results.

The envelope scattering due to secondary peaks of the spectrum can become dominant if the perturbation damps along its propagation. To study this effect, the expression (5) is multiplied by the damping term $\exp(-x_f/x_d)$, where x_d is the damping length.

4.1. Damping effect.

The results for the case of small wavenumbers, $k_f < 2k_A$, for example $k_f = 0.05k_0$, are very close to the results of the section 3.1, since the response is localized near the cut-off where damping is negligible. In the opposite case, $2k_A < k_f < 2k_0$, the influence of damping is strong. The results are shown on Figures 6 and 7, for $L = 1000\lambda_0$, $k_f = 0.6k_0$ and $x_d = 50\lambda_0$. The more the scattering corresponds to a Bragg rule far from the cut-off, the more its effect is decreased. For a Gaussian, only a weak phase variation is seen near the cut-off.

4.2. Comparison with the experimental results.

The code has been run with parameters of the above-mentioned experiment (Baang *et al* 1990, Rhodes *et al* 1992). The excitation of the ion acoustic pulse produces a modulated wavetrain of the type (5b). Figure 8 displays the phase responses corresponding to a set of values of k_f. Note that the principal response occurs always when the perturbation reaches the cut-off, that is, there is no response delay whatever the value of k_f. Figure 9 gives the computed phase amplitude as a function of k_f, for the Gaussian and the wavetrain. The experimental values taken from Rhodes *et al* (1992) have been superimposed for comparison. There is a good agreement between the experiment and the

wavetrain results for all values of k_f. We emphasize that this agreement is due to the fact that the excited wavetrain (i) has a broad spectrum with sharp edge effects and (ii) is strongly damped, so that the phase variation due to Bragg scattering near x_B vanishes. The experimental variation of the gradient length (non-linear density profile) pushes the Bragg position x_B away from the cut-off, which further increases the damping effects.

5. Tokamak fluctuation diagnostic.

The previous sections were devoted to the study of a specific perturbation, localized both in space and time, and monochromatically modulated. The situation of a tokamak experiment is very different, since the fluctuations are generally not localized. The tokamak fluctuation spectrum is usually broad both in wavenumber (≥ 1 cm^{-1}) and frequency (≥ 100 KHz), i.e. it is turbulent. The amplitude $\delta n_0/n$ varies from 10^{-3}-10^{-2} at the center up to 10-50% near the plasma edge (Liewer 1985). For the Tore Supra tokamak, coherent laser scattering measurements (Devynck *et al.* 1993) show that the k-spectrum of density fluctuations is concentrated below a critical value $k_{cr} \approx 5$ cm^{-1} and decreases as k^{-3} for $k > k_{cr}$. This behavior seems to be general for all tokamaks.

One then may ask whether fluctuation reflectometry measurements can be localized. We have shown in Section 3.1 that all fluctuations with $k < 2k_A$ produce a phase response localized at the cut-off (due to the cut-off oscillation). Larger wavenumbers produce backscattering of the incident wave at a position x given by Eq. (13). One can define the width of the cut-off layer as the distance Δx of the nearest point (from the cut-off) for which the WKB assumption is satisfied; this gives roughly $(k_0^2 L^{-1})^{1/3}\Delta x \approx 5$. Then the scattering process may be said to occur in the cut-off layer as long as the local Bragg rule, Eq. (13) is satisfied for $|x - x_c| < \Delta x$. This sets an upper limit for the critical wavenumber, $k_{cr0} = 2.42\, k_0\, (L/\lambda_0)^{-1/3}$. In other words, the scattering process is roughly localized in the cut-off layer as long as the critical wavenumber satisfies the inequality

$$k_{cr} < k_{cr0} = 2.42\, k_0\, (L/\lambda_0)^{-1/3} \tag{16}$$

To be more specific, let us consider the case of the Tore Supra spectrum ($k_{cr} \approx 5$ cm^{-1}) and a parabolic density profile

$$n(x) = n_0\left[1 - \left(\frac{x}{a}\right)^2\right] \tag{17}$$

where the minor radius $a = 70$ cm. On Fig. 10 the characteristic wavenumbers k_{cr}, $2k_A$ and k_{cr0} have been plotted versus the incident frequency for two values of the central density, $n_0 = 6\text{-}10\times10^{19}$ m^{-3}. It is clear that the condition (16) is always satisfied, thus the fluctuation reflectometry gives measurements localized in the cut-off layer. For a quantitative study of the localization problem of reflectometry, in addition to the spectrum distribution effect discussed above, we should take into account the effect due to the spatial distribution of the density fluctuations and the swelling of the incident wave close to the cut off.

6. Two-D numerical model for radial fluctuations.

Two-dimensional codes are necessary for the study of azimuthal fluctuations. In this paper, we will only check the influence of geometrical effects on the phase shift due to radial fluctuations.

In the 2-D code we have designed, the incident wave is emitted by a waveguide and a standard horn. The boundary condition at the edge of the waveguide corresponds to the fondamental waveguide mode. The numerical procedure uses a finite difference scheme with a fourth order method. In order to minimize spurious reflections, we use at the grid boundary the finite difference equations due to Higdon (1986). The solution is then computed over a box of $50\lambda_0$ (radial) $\times$ $10\lambda_0$ (azimuthal), using a biconjugate gradient method (Press 1992). The length of the box in the radial direction is large enough to ensure that the SWR in the emitting waveguide keeps a low value. The plasma has a linear density profile with a gradient length $L = 37\lambda_0$.

Since we focus on physical effects, we do not want phase modifications that could be introduced by a recepting horn, so we determine the phase shift as in the 1D model, i.e. we measure the change in the position of reflected wavefronts with respect to a reference point located on the left side of the box and $2.5\lambda_0$ below the middle axis (Figure 11). We present here results for radial fluctuations with a Gaussian envelope, with $w_f = 6\lambda_0$. The relative amplitude is now $\delta n_0/n_{cr} = 0.03$. Two cases have been studied. In the first case, the fluctuation wavenumber is constant, $k_f = 1.4k_0$. The position of the Bragg resonance is $x_B = 26\lambda_0$. In the second case the wavevector is chirped and is such that for a particular position of the fluctuation ($x_f = x_{f0} = 26\lambda_0$), the Bragg condition is satisfied everywhere. The density perturbation in this case is

$$\delta n(x) = \delta n_0 \exp[-(x - x_f)^2/w_f^2] \cos[k_f(x)(x - x_f)],$$

$$k_f(x) = 2\left(1 - \frac{x - x_f + x_{f0}}{L}\right)^{1/2} \qquad (18)$$

Because of large computation time, the 2-D phase response has been computed only near its maximum and near one of the edges. Figure 12 displays the results of the first case. As the gradient length is small, the phase response is in the spatial regime (as on Figure 4a). As expected, the modulation length is constant and corresponds to the local wavelength at $x \approx x_B$.

The case of a chirp is shown on Figure 13. The chirp of k_f introduces a variation of the modulation length with x_f.

From the very good agreement between the 1-D and 2-D results, we can infer that the role of geometry effects is negligible for radial fluctuations. Therefore, one-dimensional models are adequate for this case.

7. Conclusions.

The phase response of a reflectometer to a quasi-monochromatic perturbation localized both in space and time has been studied in details in this paper, with a one-dimensional code and several asymptotic formulae. The roles of the physical processes involved (oscillation of the cut-off layer and Bragg backscattering) are clearly exhibited. The phase response is strongly influenced by the shape of the perturbation. There are basically two situations:

a) $k_f < 2k_A$, the Bragg selection rule cannot be satisfied, the phase response is localized in the cut-off layer and is due to the cut-off layer oscillation.

b) $k_f > 2k_A$, the resonant Bragg scattering is dominant. Two different regimes exist, depending upon the relative width of the perturbation. In the spatial regime, the phase response reproduces the spatial shape of the perturbation. In the spectral regime, the phase response reproduces the spectral shape of the perturbation; scattering may occur at locations that are far from the Bragg position. Furthermore, signals with sharp envelope boundaries produce a significant phase response at the cut-off.

To understand the origin of the discrepancy between the previous code results and the experimental observations, a damped wavetrain (a square envelope sinusoidally modulated) has been used in the code to simulate the ion acoustic wavepacket. The agreement then becomes quite satisfactory between the code and the experiment. The reason is that such a damped wavetrain with sharp boundaries has a broad spectrum and produces a phase response which is dominant at the cut-off.

In order to check the role of geometrical effects for radial fluctuations, a two-dimensional code has been developed. The 1D and 2D codes have been run for the same physical system (a modulated Gaussian perturbation). It turns out very clearly that the phase response is very insensitive to two-dimensional effects.

The application of these results to fluctuation reflectometry in a tokamak leads to the conclusion that, assuming a universal behavior for the fluctuation spectra, with a strong decay of the spectra above some critical value of k, the reflectometry diagnostic should bring information on those fluctuations that are localized near the cut-off layer.

Appendix A. Scattering in the WKB region

In the Born approximation, the phase variation due to the scattering of the incident wave by a density perturbation $(\delta n_0/n_{cr})f(\xi)$ is (Afeyan et al 1995)

$$\Delta\phi = -\,2\pi k_0 L^{2/3}\,\frac{\delta n_0}{n_{cr}}\int d\xi\; f(\xi)\;Ai^2(\xi) \tag{A1}$$

where $\xi = x(L^{-1}k_0^2)^{1/3}$. Let us consider the case where the scattering occurs away from the cut-off layer, so that the WKB approximation is valid. With the asymptotic expansion of the Airy function, Eq.(A1) becomes

$$\Delta\phi = -\,2k_0 L^{1/2}\,\frac{\delta n_0}{n_{cr}}\int dx\; f(x)\,\frac{\cos[k_f(x-x_f)]}{x^{1/2}}\,\sin^2\left[\tfrac{4}{3}k_0 L^{-1/2}x^{3/2} + \pi/4\right] \tag{A2}$$

This expression can be split into two integrals

$$\Delta\phi = -\,k_0 L^{1/2}\,\frac{\delta n_0}{n_{cr}}\left\{\int dx\,\frac{f(x)}{x^{1/2}}\cos[k_f(x-x_f)] + \int dx\,\frac{f(x)}{x^{1/2}}\sin\left[\tfrac{4}{3}k_0 L^{-1/2}x^{3/2}\right]\right\} \tag{A3}$$

The first integral corresponds to the phase modulation experienced by the incident wave as it propagates through the fluctuating region (i.e. forward scattering). The second integral corresponds to Bragg backscattering. We evaluate this second integral for a modulated Gaussian perturbation

$$f(x) = \exp\left[-\,\frac{(x-x_f)^2}{w_f^2}\right]\cos[k_f(x-x_f)]$$

The second part of expression (A3) can be rewritten as

$$\Delta\phi = \frac{i}{4}\,k_0 L^{1/2}\,\frac{\delta n_0}{n_{cr}}\int dx\,\exp\left[-\,\frac{(x-x_f)^2}{w_f^2}\right]\frac{1}{x^{1/2}}\left[e^{ip(x)} + e^{iq(x)}\right] + c.c \tag{A4}$$

where *c.c* stands for complex conjugate and

$$p(x) = \tfrac{4}{3}\,k_0 L^{-1/2}\,x^{3/2} + k_f(x - x_f), \qquad q(x) = \tfrac{4}{3}\,k_0 L^{-1/2}\,x^{3/2} - k_f(x - x_f)$$

Let us first assume that the phases $p(x)$ and $q(x)$ are rapidly varying functions over the width w_f of the Gaussian, i.e. $q(x_f+w_f) - q(x_f) \gg 1$. In the WKB region, $x_f, x_B \gg w_f$, this condition is $w_f^2 \gg Lk_f/k_0^2 = w_c^2$. This is the condition for the spatial regime with wide perturbations. Thus an asymptotic evaluation of the integral in (A4) can be immediately obtained by the method of stationary phase (Murray 1984)

$$\int dt\ g(t)\ \exp[ih(t)] \approx (2\pi)^{1/2}\ g(a)\frac{\exp\{i[h(a) + \pi/4\ \mathrm{sgn}(h''(a))]\}}{|h''(a)|^{1/2}} \qquad \text{(A5)}$$

where a is the stationary phase point, $h'(a) = 0$. In our case the stationary phase point results from the $q(x)$ term. It merely states the Bragg rule

$$x = \frac{L}{4k_0^2} k_f = x_B \qquad \text{(A6)}$$

From (A5) and (A4), one finds the phase response

$$\Delta\phi \approx \pi\sqrt{2}\left(\frac{k_0}{k_f}\right)^{1/2}\left(\frac{L}{\lambda_0}\right)^{1/2} \exp\left[-\frac{(x_f - x_B)^2}{w_f^2}\right] \sin(k_f x_f + \psi_0) \qquad \text{(A7)}$$

where $\psi_0 = \frac{4}{3} k_0 L^{-1/2} x_B^{3/2} - k_f x_B + \pi/4$

In other words, in this case the phase response as a function of x_f reproduces the spatial characteristics of the perturbation, as already found by Afeyan et al (1995)

For narrow enough perturbations the stationary phase evaluation of (A4) cannot be used. Instead we introduce the wavenumber spectrum of the Gaussian envelope

$$\int dx\ \exp[-\frac{(x - x_f)^2}{w_f^2}]\ e^{-i\chi x} = \sqrt{\pi}\, w_f \exp\left[-\tfrac{1}{4}\chi^2 w_f^2\right] \exp(-i\chi x_f)$$

and rewrite (A4) as

$$\Delta\phi = \frac{i}{8\pi^{1/2}} k_0 w_f L^{1/2} \frac{\delta n_0}{n_{cr}} \int d\chi\ \exp\left[-\tfrac{1}{4}\chi^2 w_f^2\right] \int dx\ \frac{1}{x^{1/2}}$$

$$\left\{\exp[iP_+(x)] - \exp[iP_-(x)] + \exp[iQ_+(x)] - \exp[iQ_-(x)]\right\} \qquad \text{(A8)}$$

$$P_\pm(x) = \pm p(x) + \chi(x - x_f), \qquad Q_\pm(x) = \pm q(x) + \chi(x - x_f)$$

The x-integral is evaluated by the stationary phase method. Only Q_+ and Q_- give significant contributions. The stationary points are

$$x = \frac{L}{4k_0^2}(k_f \pm \chi)^2 \qquad \text{(A9)}$$

which leads to the following expression of the phase shift

$$\Delta\phi = \frac{i}{4} k_0 w_f L^{1/2} \frac{\delta n_0}{n_{cr}} \int d\chi\ \exp\left[-\tfrac{1}{4}\chi^2 w_f^2\right] \frac{1}{(k_f \pm \chi)^{1/2}} |e^{i\vartheta_+} + e^{i\vartheta_-}| \qquad \text{(A10)}$$

$$\vartheta_\pm = \mp\left[\frac{1}{12}\frac{L}{k_0^2}(k_f \pm \chi)^3 - (k_f \pm \chi)x_f - \pi/4\right]$$

The χ-integrals can be evaluated by the stationary phase method if the phase $\vartheta_{\pm}$ in the imaginary exponentials vary rapidly over the width $2/w_f$ of the Gaussian, say, $\vartheta_{\pm}(\chi = 2/w_f) - \vartheta_{\pm}(\chi = 0) \gg 1$. In the WKB region, this leads to the condition for the spectral regime of narrow perturbations, $w_f \ll w_c$. The asymptotic evaluation of the χ-integrals involves the stationary points

$$\chi \pm k_f = 2k_0 \frac{x_f^{1/2}}{L^{1/2}} \tag{A11}$$

Finally, the phase response for narrow pulses is given by

$$\Delta\phi = -\frac{\pi^{1/2}}{2} k_0 w_f \frac{\delta n_0}{n_{cr}} \left(\frac{L}{x_f}\right)^{1/2} \exp\left[-\frac{k_0^2 w_f^2}{L}(x_f^{1/2} - x_B^{1/2})^2\right] \sin\left[\frac{4}{3}\frac{k_0}{L^{1/2}} x_f^{3/2}\right] \tag{A12}$$

It results that the width of the phase response is now related to the width of the Fourier transform of the Gaussian perturbation and its modulation wavelength varies continuously according to a local Bragg rule. Due to the nonlinear dependence of this Bragg rule, the envelope of the response is no longer a Gaussian in the real space. The characteristic width W of the phase response may be estimated by setting

$$\frac{k_0^2 w_f^2}{L}\left[(x_B \pm W)^{1/2} - x_B^{1/2}\right]^2 \approx 1$$

which gives

$$W \approx L \frac{k_f}{k_0} \frac{1}{w_f k_0} \tag{A13}$$

Hence, the critical width w_c corresponds to a perturbation having a width w_f equal to the width W of its Fourier transform.

Appendix B. Phase response of a modulated Square pulse near the cut--off.

Let us consider here the wavetrain in the form:

$$\delta n = \delta n_0 \sin[k_f(x - x_f + w_f)] , \qquad x > x_f - w_f , \quad x < x_f + w_f$$

which ensures a smooth start of the signal at $x = x_f - w_f$. The phase variation in the Born approximation is related to the integral (Afeyan et al 1995):

$$I = \delta\nu_0 \int_{\xi_f - \Lambda}^{\xi_f + \Lambda} d\xi \sin[\kappa_f(\xi - \xi_f + \Lambda)] \, Ai^2(\xi) \qquad \text{(B1)}$$

where ξ is the variable that transforms the wave equation into an Airy equation, $\delta\nu_0$, κ_f et Λ are the corresponding values of δn_0, k_f et w_f. Letting $\eta = \xi - \xi_f + \Lambda$ one has

$$I = \delta\nu_0 \int_0^{2\Lambda} d\eta \sin(\kappa_f\eta) \, Ai^2(\eta + \xi_f - \Lambda)$$

This can be rewritten as

$$I = \lim_{a\to 0} \delta\nu_0 \int_a^{2\Lambda} d\xi \sin[\kappa_f(\eta - a)] \, Ai^2(\eta + \xi_f - \Lambda) = \lim_{a\to 0} I_a \qquad \text{(B2)}$$

We are looking at effects near the cut-off, $\xi_f \lesssim \xi_c$. Assuming that the pulse is long enough, $\xi_f + \Lambda > \xi_c$, $Ai^2(\xi_f + \Lambda) \approx \exp[-2/3(\xi_f + \Lambda)^{3/2}] \approx 0$, we obtain the equation satisfied by I_a

$$\frac{\partial^2 I_a}{\partial a^2} + \kappa_f^2 I_a = \kappa_f Ai^2(\xi_f - \Lambda + a)$$

In the $\kappa_f \gg 1$ limit, assuming that $\partial^2 I_a/\partial a^2$ and I_a are of the same order the approximate solution is

$$I_a = \frac{\delta\nu_0}{\kappa_f} Ai^2(\xi_f - \Lambda + a) \qquad \text{(B3)}$$

Near the cut-off (B3) verifies the previous assumption. It results that

$$I = \frac{\delta\nu_0}{\kappa_f} Ai^2(\xi_f - \Lambda) \qquad \text{(B4)}$$

Going back to the physical variables, Eq. (B4) leads to Eq. (8).

References

AfeyanB.B., Chou A.E. and Cohen B.I. 1995, *Plasma Phys. Control. Fusion* **37**, 315

Baang S, Domier C W, Luhmann N C, Peebles W A and Rhodes T L 1990
Rev. Sci. Instrum. **61** 3013

Bretz N. 1992, *Phys. Fluids* B **4**, 2414

Carnahan B., Luther H.A. and Wilkes J.O. 1969, *Applied Numerical Methods*,
John Wiley, New York

Devynck P., Garbet X., Laviron C., Payan J., Saha S. K., Gervais F., Hennequin P.,
Quéméneur A. and Truc A. 1993, *Plasma Phys. Control. Fusion* **35**, 63

Hanson G.R., Harris J.H., Wilgen J.B., Thomas C.E., Aceto S.C., Baylor L.R., Bell J.D.,
Branas B., Dunlap J.L., England A.C., Hidalgo C., Murakami M., Rasmussen D.A.,
Sanchez Sanz J., Schwelberger J.G., Uckan T. and Zielinski J.J. 1992, *Nucl. Fusion* **32**, 1593

Higdon R.L. 1986 *Math. Comp.* **47**, 437

Hutchinson I.H. 1992, *Plasma Phys. Control. Fusion* **34**, 1225

Irby J.H., Home S., Hutchinson I.H. and Steck P.C. 1993,
Plasma Phys. Control. Fusion **35**, 601

Kramer G.J., Sips A.C.C. and Lopes Cardozo N.J. 1993,
Plasma Phys. Control. Fusion **35**, 1685

Liewer P. C. 1985, *Nucl. Fusion* **25**, 543

Manso M.E. 1993, *Plasma Phys. Control. Fusion* **35**, B141

Mazzucato E. and Nazikian R. 1991, *Plasma Phys. Contr. Fusion* **33**, 261

Murray J. (1984), *Asymptotic Analysis*, Springer Verlag, New York

Press W H, Teukolsky S A, Vetterling W T and Flannery 1992
Numerical Recipes 2nd ed. (Cambridge University Press)

Rhodes T.L., Baang S., Chou A.E., Domier C.W., Luhmann N.C., Jr, and Peebles W.A. 1992,
Rev. Sci. Instrum. **63**, 4599

Simonet F. 1985, *Rev. Sci. Instrum.* **56**, 664

Zou X.L., Laurent L. and Rax J.M. 1991, *Plasma Phys. Contr. Fusion* **33**, 903

Figure captions

Figure 1 - Gaussian and Square perturbations (a and b) and their spectra (c and d). x_f is the center of the perturbation, w_f its half-width, and k_f its modulation wavenumber.

Figure 2 - Phase response versus the position x_f of the perturbation. Case of a long wavelength Gaussian perturbation, $k_f = 0.04k_0$. $L = 1000\lambda_0$, $w_f = 50\lambda_0$.

Figure 3 - Phase response versus the position x_f of the perturbation. Case of a long wavelength Square perturbation, $k_f = 0.04k_0$. $L = 1000\lambda_0$, $w_f = 50\lambda_0$.

Figure 4 - Phase response (solid line) versus the position x_f of the perturbation. Case of a Gaussian perturbation, $k_f = 0.4k_0$. $L = 1000\lambda_0$. a) Spatial case, $w_f = 15\lambda_0$. b) Spectral case, $w_f = 2.5\lambda_0$. The dotted line corresponds to the asymptotic formulae (10) or (12). The bold solid line represents the perturbation envelope centered at $x_f = x_B$.

Figure 5 - Phase response versus the position x_f of the perturbation. Case of a Square perturbation, $k_f = 0.6k_0$. $L = 1000\lambda_0$. a) Spatial case, $w_f = 30\lambda_0$. b) Spectral case, $w_f = 5\lambda_0$. The bold solid line represents the perturbation envelope centered at $x_f = x_B$.

Figure 6 - Damped Gaussian perturbation. Phase response versus the position x_f of the perturbation. $k_f = 0.6k_0$, $L = 1000\lambda_0$, $w_d = 50\lambda_0$. a) Spatial case, $w_f = 15\lambda_0$. b) Spectral case, $w_f = 2.5\lambda_0$.

Figure 7 - Damped Square perturbation. Phase response versus the position x_f of the perturbation. $k_f = 0.6k_0$, $L = 1000\lambda_0$, $w_d = 50\lambda_0$. a) Spatial case, $w_f = 30\lambda_0$. b) Spectral case, $w_f = 5\lambda_0$.

Figure 8 - Phase response versus the position x_f of a damped wavetrain for a set of values of k_f. Parameters as in Rhodes *et al* 1992.

Figure 9 - Maximum phase response versus the wavenumber k_f. Parameters as in Rhodes *et al* 1992.
× and + : numerical results for the damped wavetrain and Gaussian respectively.
: experimental points taken from Rhodes *et al* (1992). Solid line : analytical expression (15).

Figure 10 - Characteristic wavenumbers k_A, k_{cr} and k_{cr0} vs the incident frequency for two typical Tore Supra plasmas: the central density n_0=6 10^{19} m^{-3} and n_0=10 10^{19} m^{-3}.

Figure 11 - Sketch of the two-dimensional wave-plasma system. The contour plots of the real part of the electric field are represented.

Figure 12 - Phase response versus the position x_f of a radial Gaussian perturbation. a) Constant fluctuation wavenumber, $k_f = k_0$. b) Chirped fluctuation wavenumber, Eq. (18).

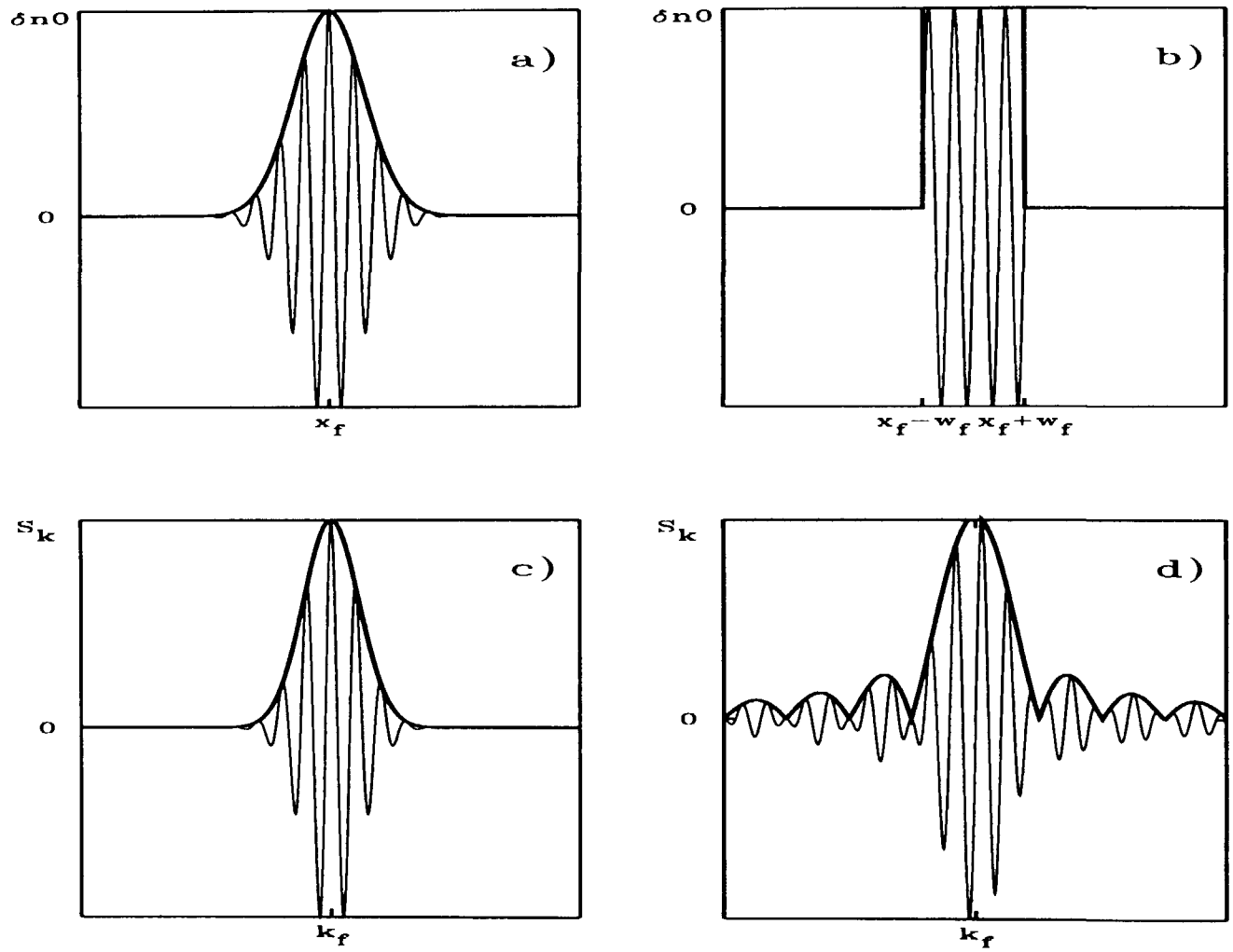

Figure 1

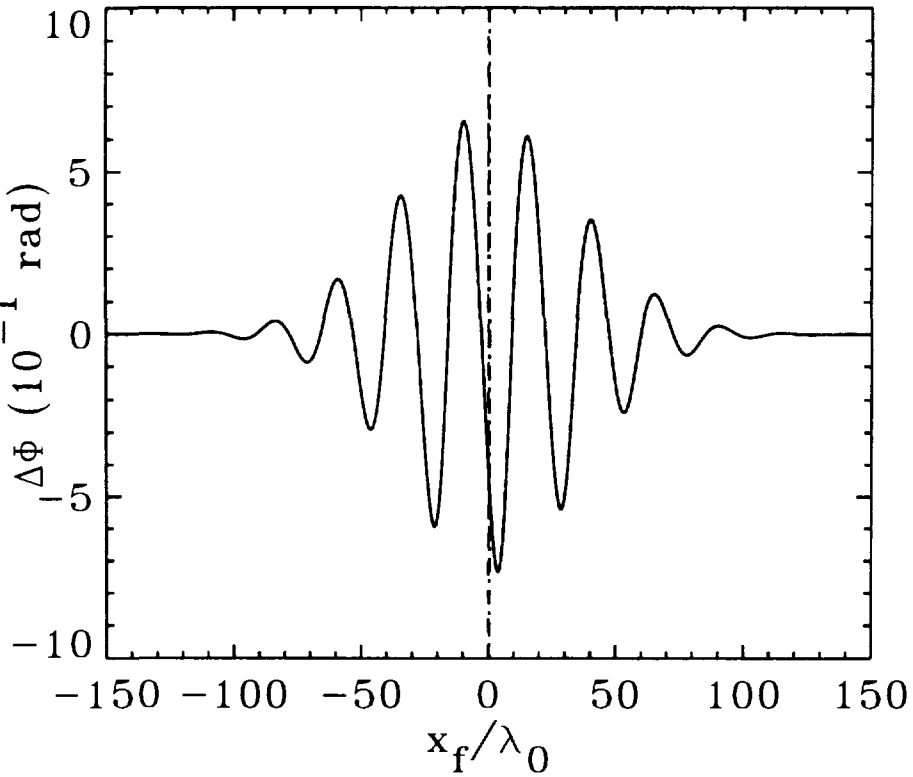
10
5
0
−5
−10
−150 −100 −50 0 50 100 150
$\Delta\Phi$ (10^{-1} rad)
x_f/λ_0

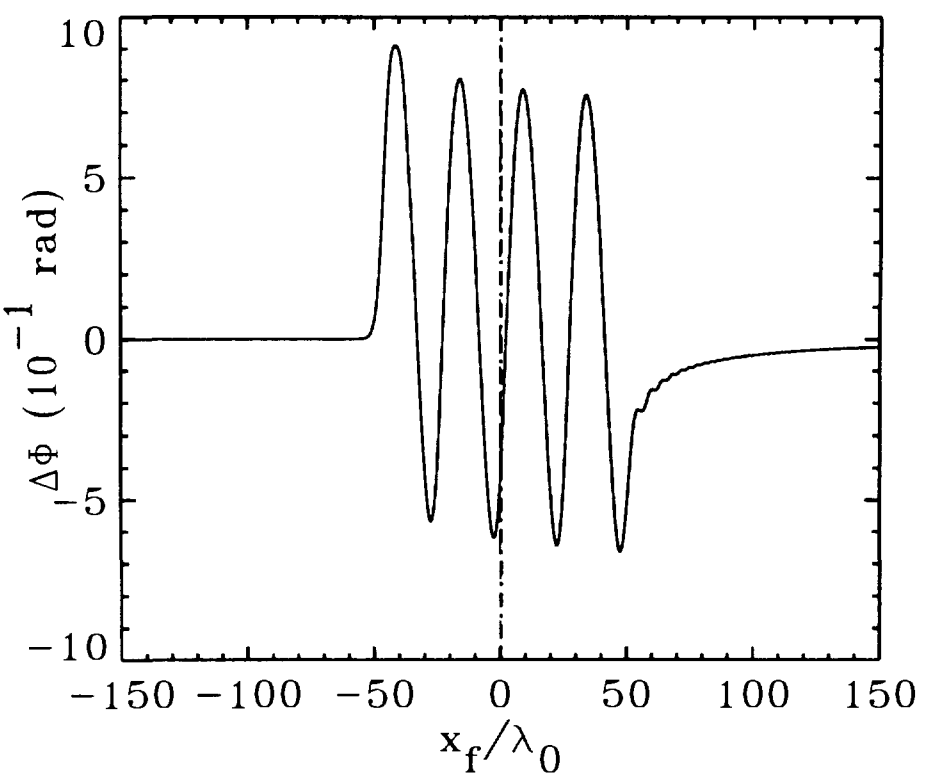
10
5
0
−5
−10
−150 −100 −50 0 50 100 150
$\Delta\Phi$ (10^{-1} rad)
x_f/λ_0

Figures 2 & 3

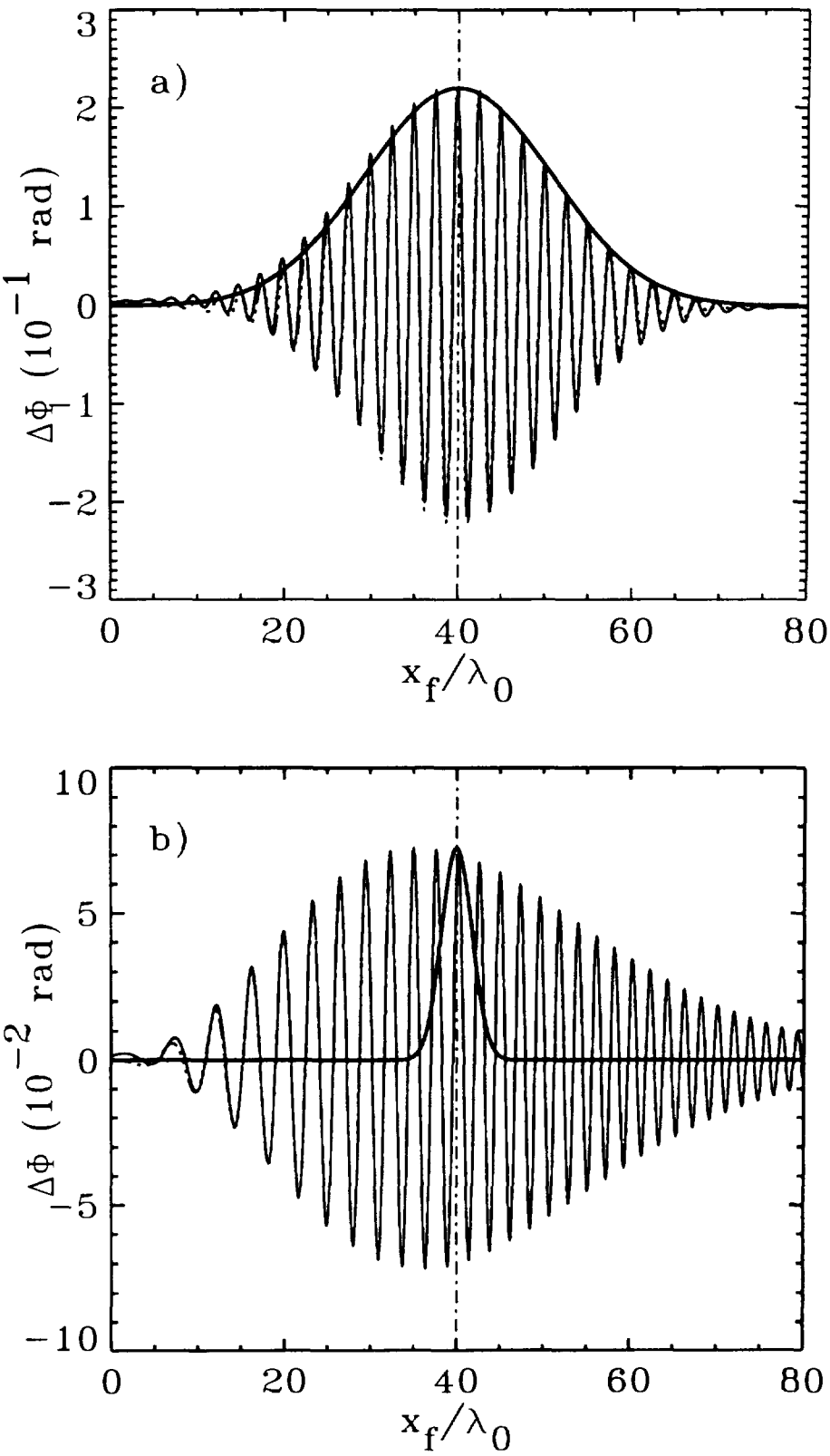

Figure 4

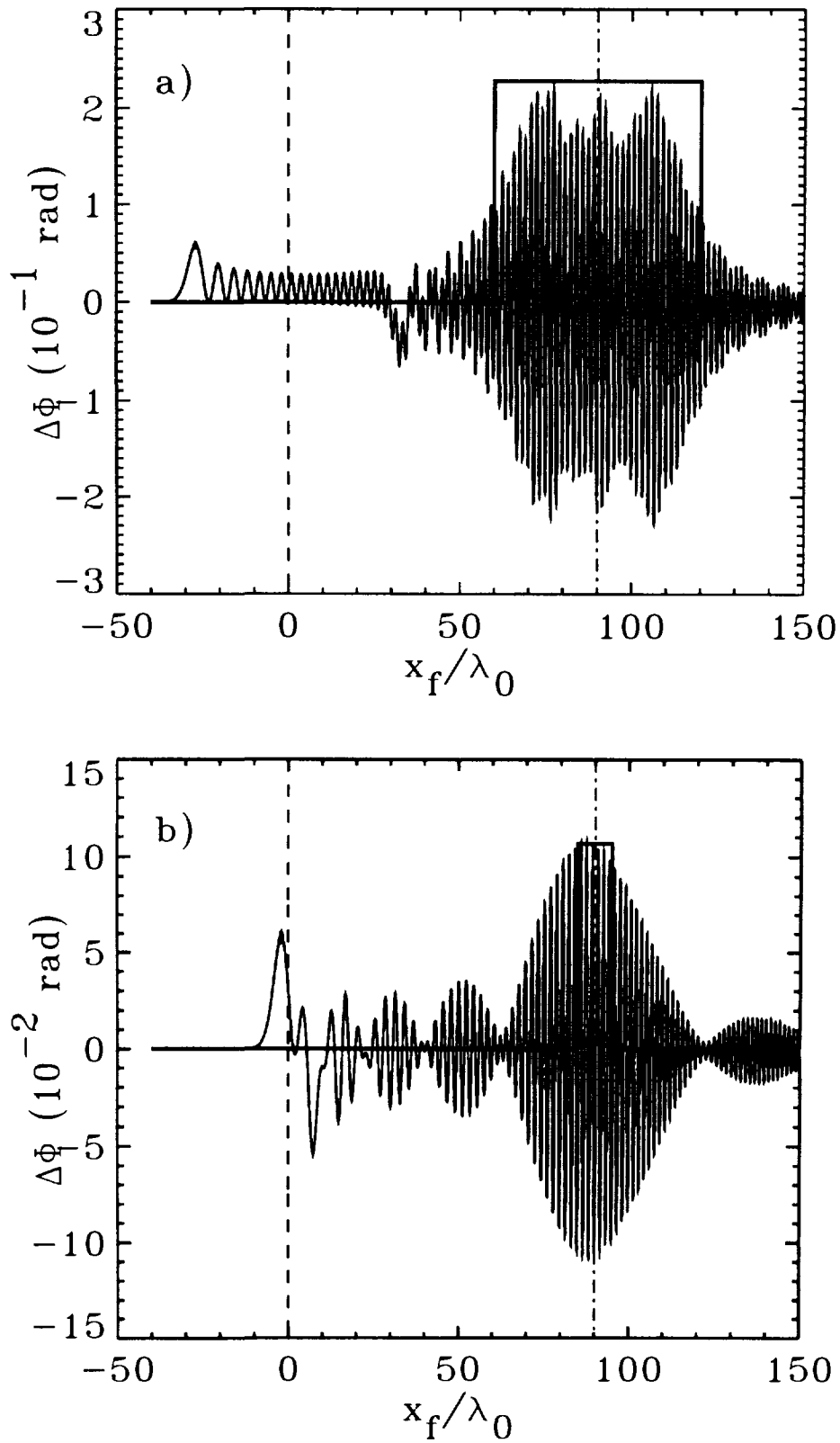
a)
b)
$\Delta\Phi_f$ (10^{-1} rad)
$\Delta\Phi_f$ (10^{-2} rad)
x_f/λ_0
x_f/λ_0

Figure 5

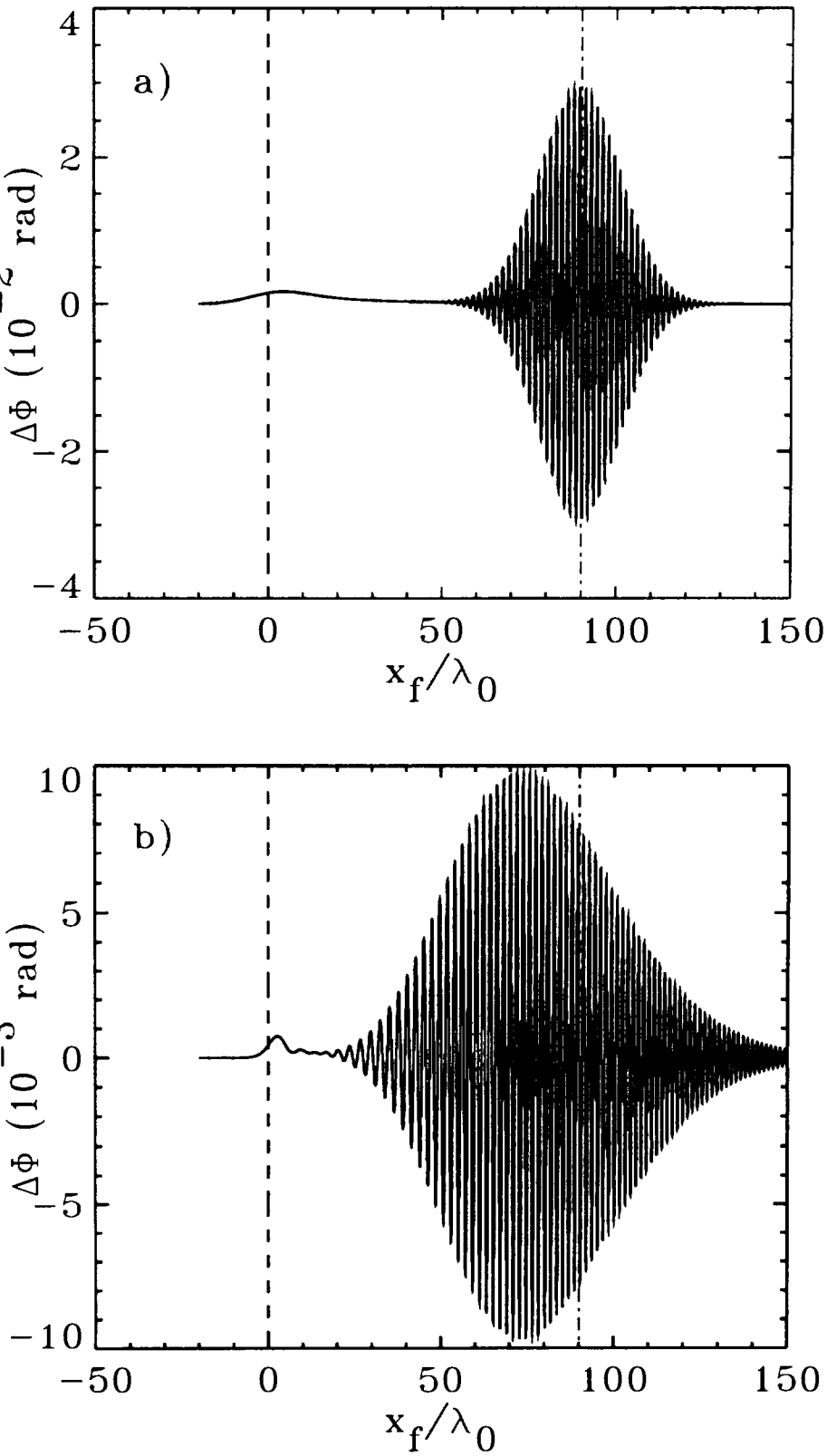

Figure 6

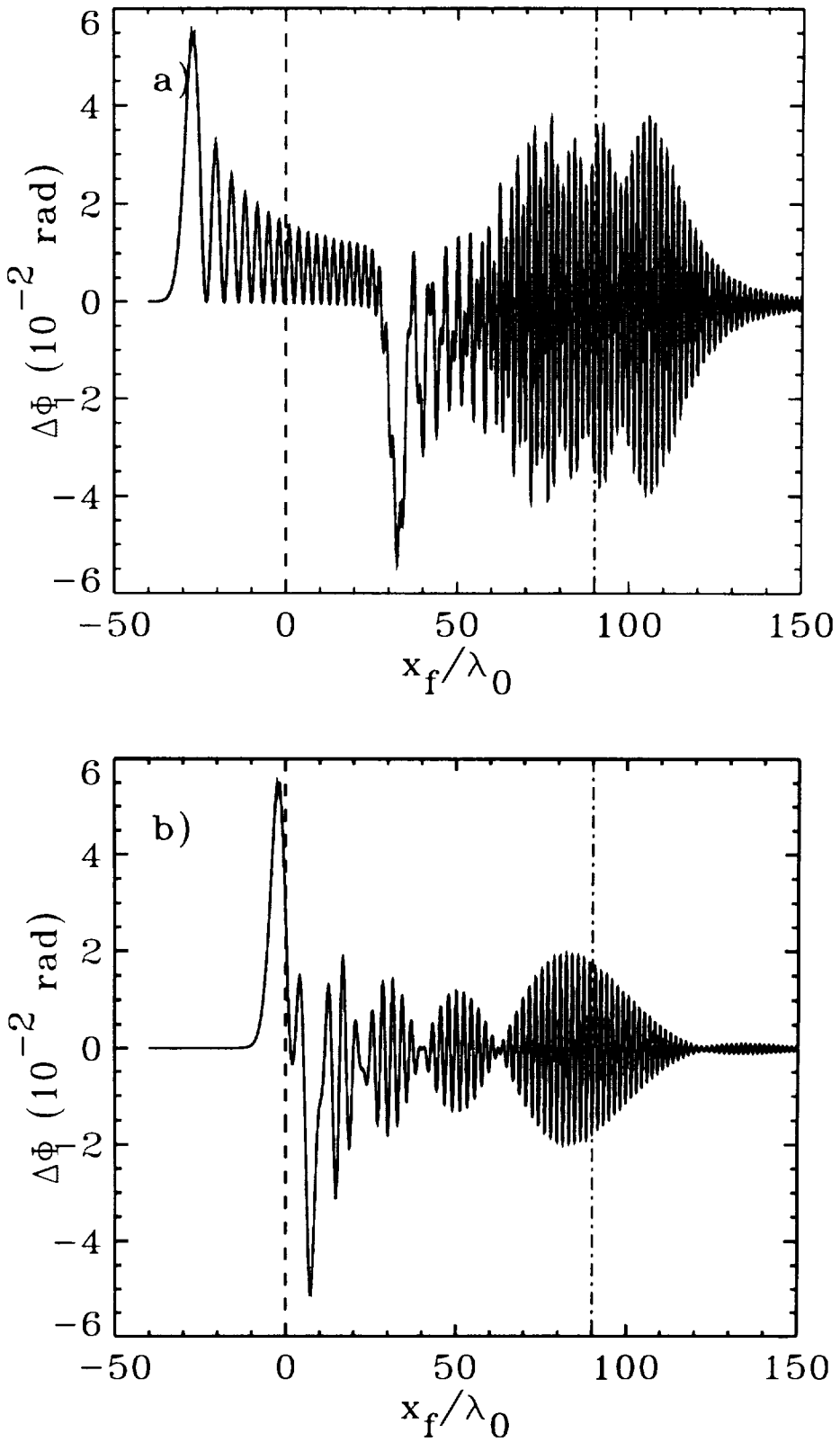

Figure 7

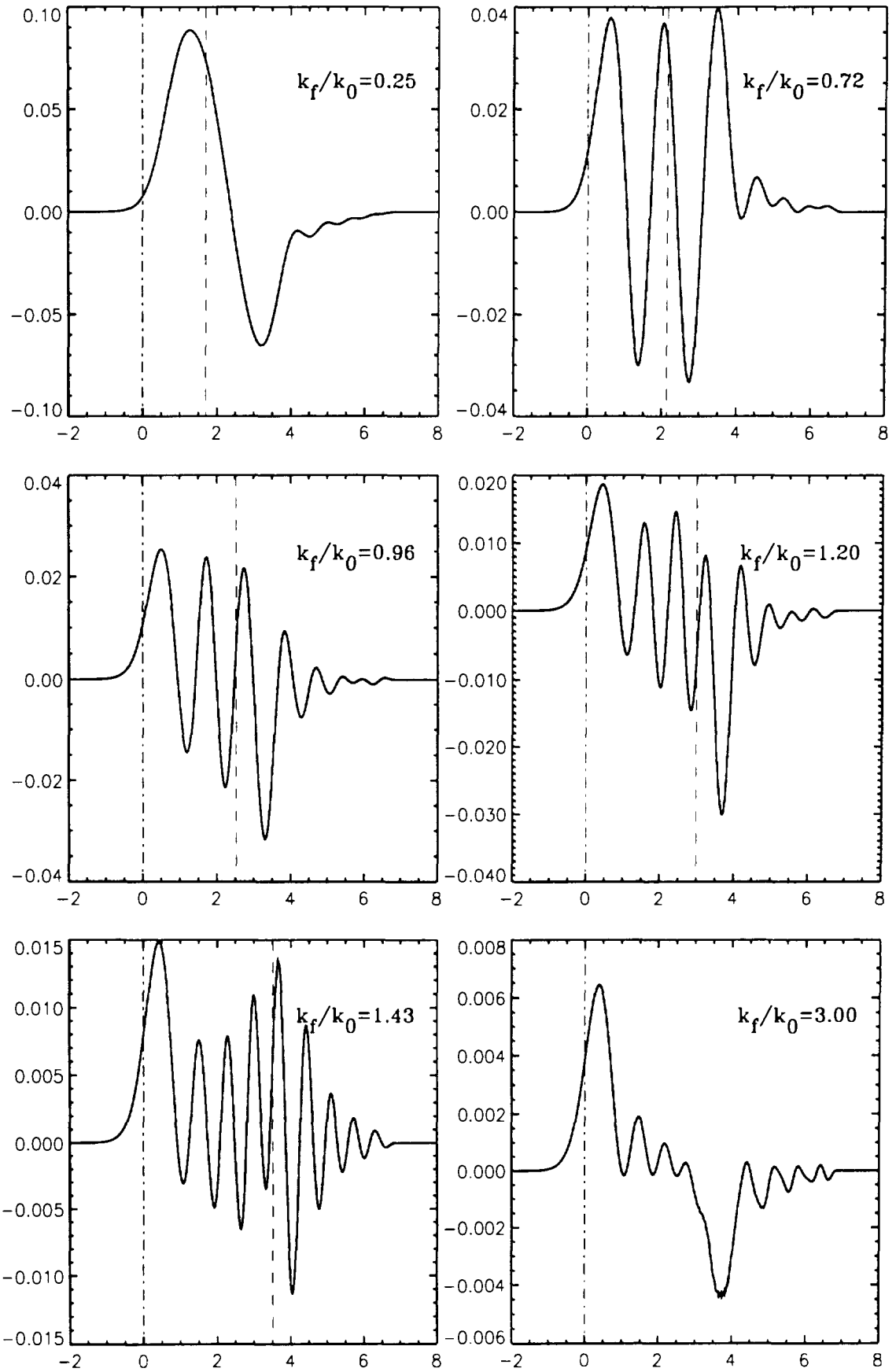

Figure 8

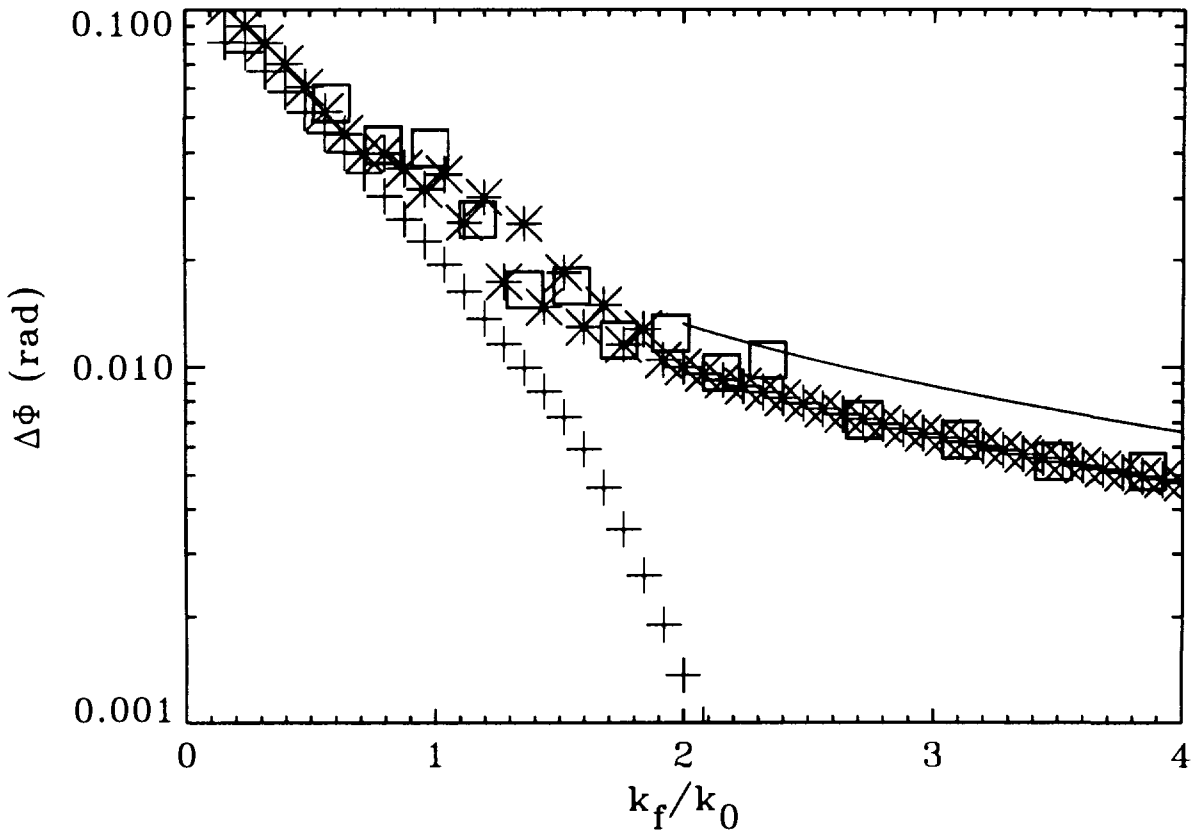

Figure 9

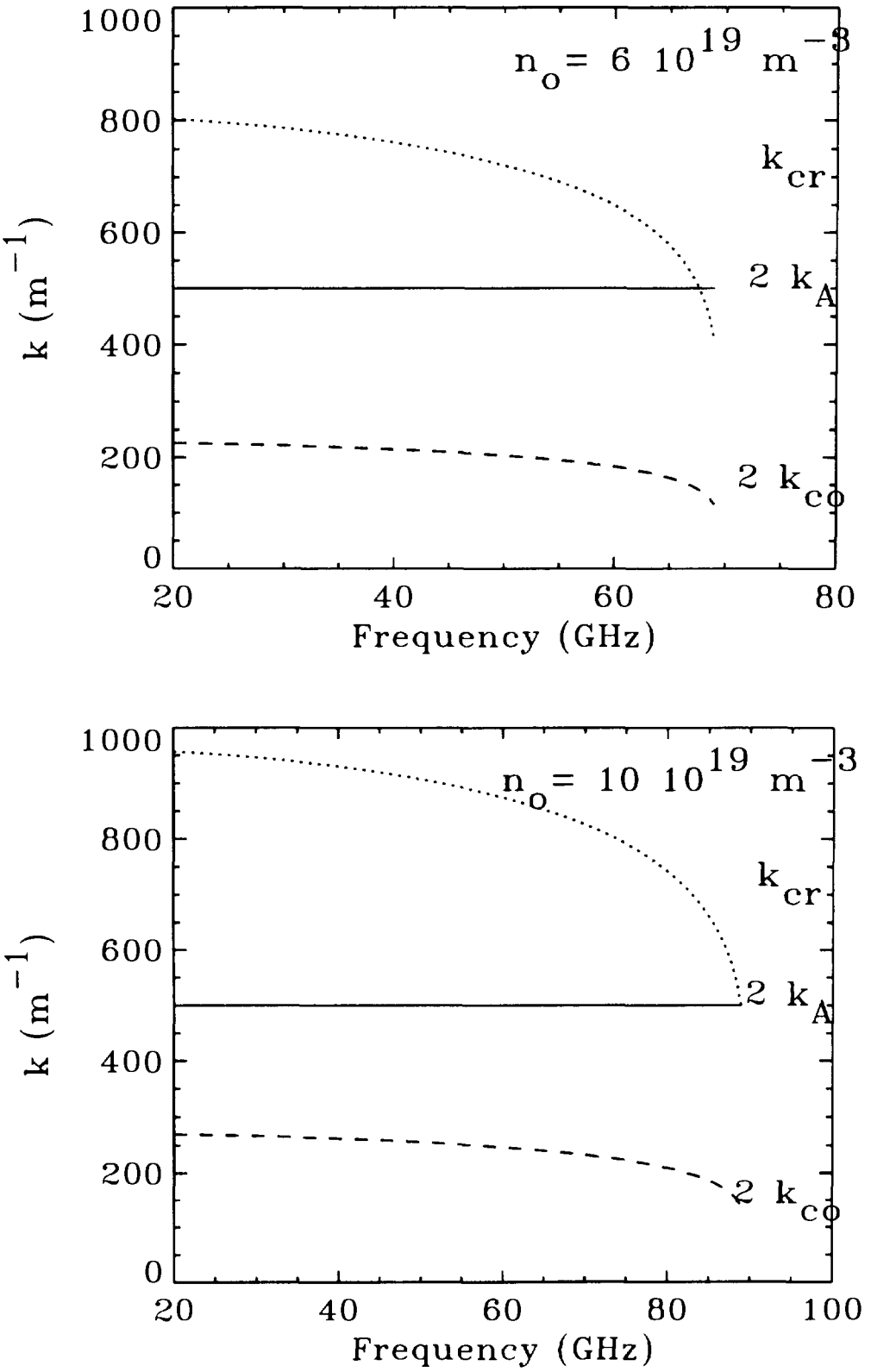
1000
800
600
400
200
0
k (m^{-1})
n_o= 6 10^{19} m^{-3}
k_{cr}
2 k_A
2 k_{co}
20
40
60
80
Frequency (GHz)
1000
800
600
400
200
0
k (m^{-1})
n_o= 10 10^{19} m^{-3}
k_{cr}
2 k_A
2 k_{co}
20
40
60
80
100
Frequency (GHz)

Figure 10

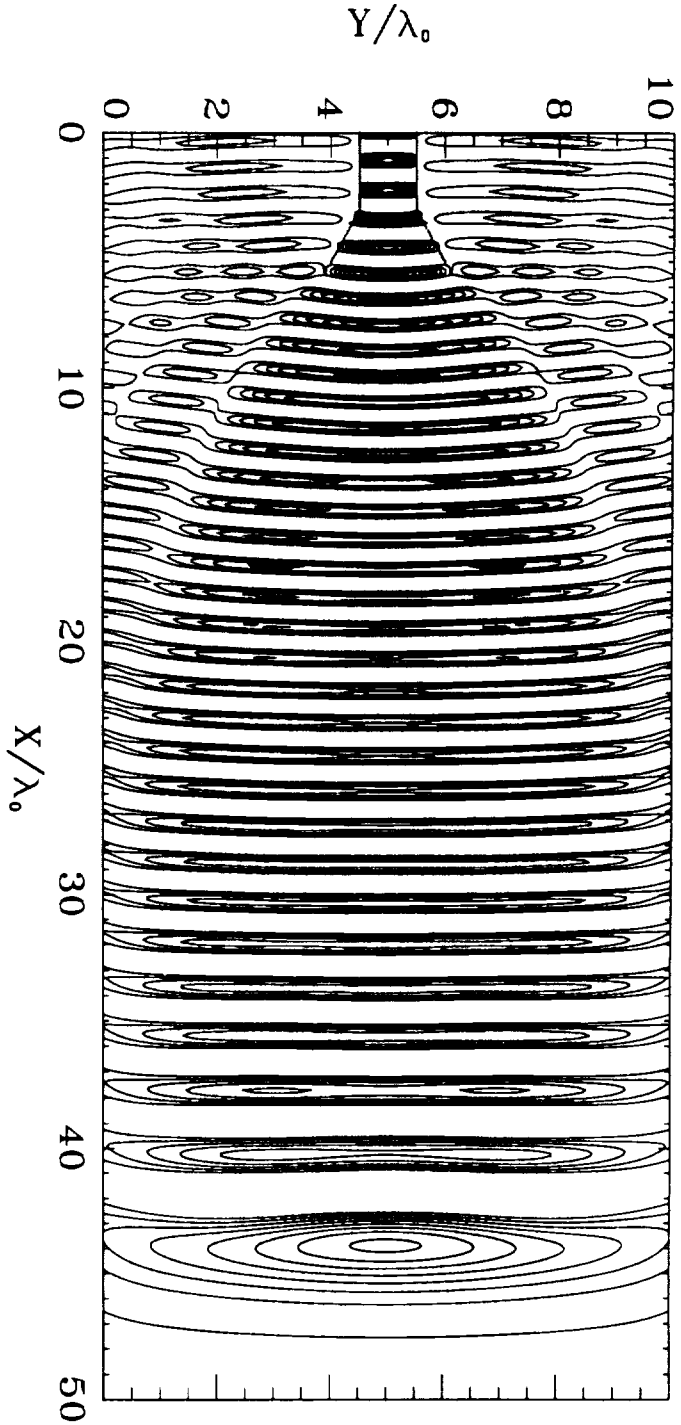

Figure 11

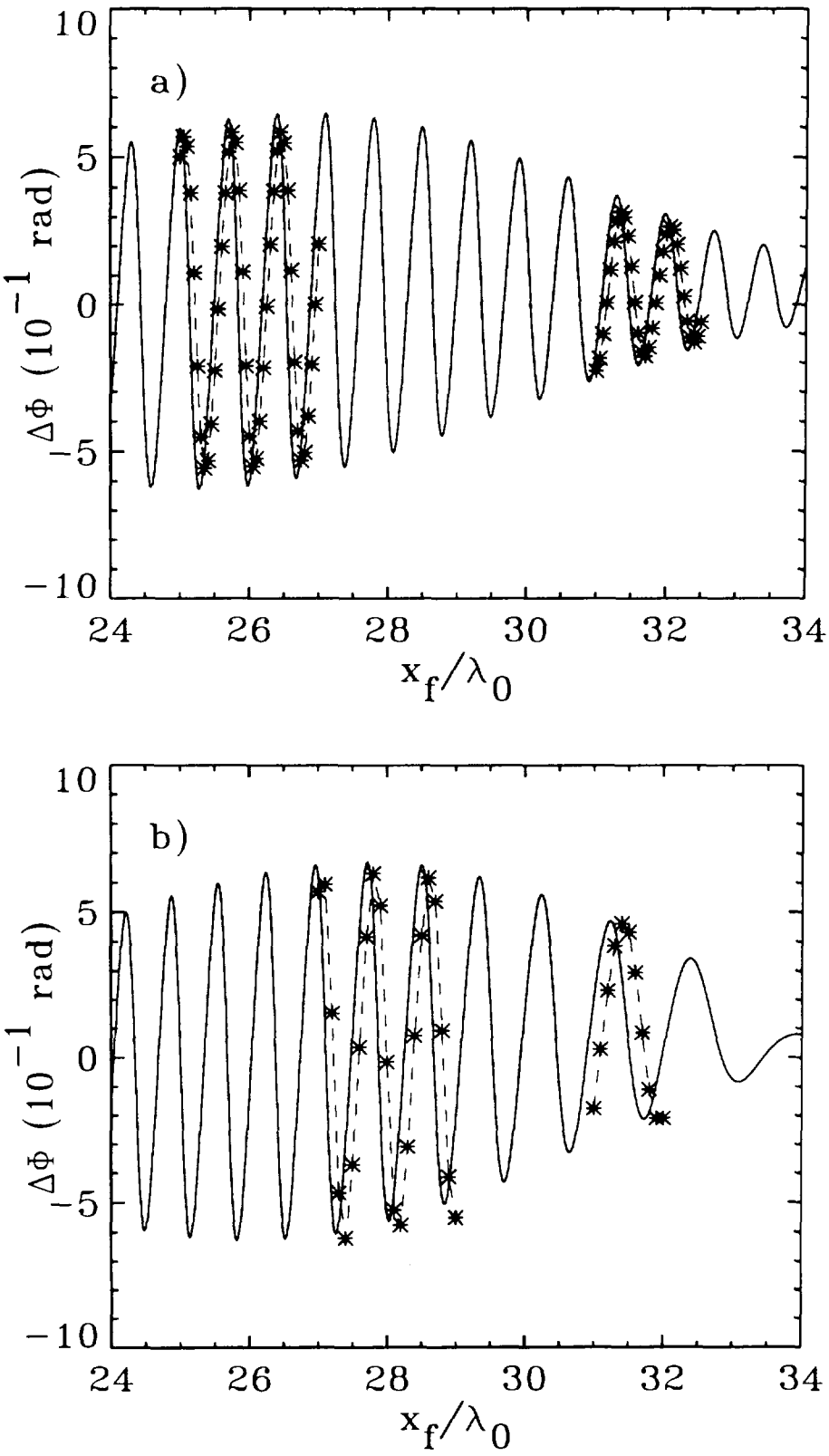

Figure 12